Single Crystal ESR of Copper Doped KHCO$_3$

Albert Lötz

Department Chemie, Universität München, Butenandtstr. 5 – 13, Haus E, D-81377 München

Reprint requests to Dr. A. L.; Fax: +49 89 2180 77622; E-mail: Albert.Loetz@cup.uni-muenchen.de

The principal components of the **g**- and **A**-tensor of ^{63}Cu^{2+} obtained from single crystal ESR spectra of copper doped KHCO$_3$ are $g_{zz} = 2.2347(1)$, $g_{yy} = 2.0474(1)$, $g_{xx} = 2.0468(1)$, $A_{zz} = 20.43(2)$ mT, $A_{yy} = 3.22(1)$ mT, $A_{xx} = 2.63(2)$ mT. The unique axes of both tensors are parallel and lie in the mirror plane of the point group of the crystal (2/m). The direction of this axis conforms with the expectation from the structure of the first coordination shell of the K$^+$ ions. This provides strong evidence for copper entering the K$^+$ positions without major lattice disturbance. Several of the results presented here are at variance with those of an earlier report on the same subject.

Key words: ESR; Cu^{2+}; Single Crystal; Potassium Bicarbonate.

Introduction

A few years ago an ESR investigation of copper doped single crystals of KHCO$_3$ was published in this journal [1]. The spectra could be recorded at room temperature and were characterized by small line widths of 1 – 2 Gauss which led to well resolved hyperfine transitions of the two copper isotopes ^{63}Cu and ^{65}Cu. The single crystals had been prepared by simple evaporation from aqueous solution. These features, and the stability of the sample, made the compound attractive for an ESR experiment in our advanced course in physical chemistry. When the spectra were recorded during the setup of the experiment, some inconsistencies with [1] became obvious. These are reported here, together with a simple interpretation.

Experimental

The spectra were recorded at X-band on a VARIAN E-Line instrument interfaced to a personal computer. The microwave frequency was measured with an EIP Model 25B counter (Phase Matrix Inc., San Jose, USA) and the magnetic field with a Metrolab NMR-teslameter PT 2025 (Metrolab Instruments SA, Geneva, Switzerland), connected to a personal computer for automatic calibration of the field axis. The g-value of the p-benzosemichinone radical anion in ethanolic solution thus found was identical with the literature value within the quoted error (± 0.00003) [2].

Single Crystals

The single crystals of edge lengths in the millimeter range were grown from an aqueous solution with a molar ratio 100/1 in KHCO$_3$/CuSO$_4$. Analysis of several combined single crystals by stripping voltammetry yielded a ratio 100/0.026. The copper content of the single crystals of [1] was not specified.

The growth habit of the monoclinic KHCO$_3$ single crystals is described in several publications. The older ones are summarized in [3]. A clear description of more recent origin was given in a paper which addressed some confusion between single crystal X-ray and Raman results [4]. The usually largest face of the crystals indexed (101) by Groth [3] had to be reindexed $(40\bar{1})$ after the first X-ray investigations. For a detailed X-ray and a neutron diffraction study see [5, 6].

The crystals were mostly obtained as plates. A cross section perpendicular to the largest face and along its longest edges had the form of a parallelogram with a sharp angle of approximately $53°$ when quite small faces were not taken into account. The two faces defining the parallelogram were assigned the $(40\bar{1})$ and the (100) faces, which form an angle of $51.50°$ according to the X-ray structure. The two-fold axis of the parallelogram then had to be the b-axis of the monoclinic structure. This assignment was confirmed by Bragg-diffraction at the $(40\bar{1})$ face, which showed a reflection at $30.6 \pm 0.5°$ (expected: $31.2°$ for the second order reflection with Cu-Kα_1-radiation). The $(40\bar{1})$ face causes the plate-like form of the crystals.

A rod of ca. 12 cm length was milled from Rexolite (Goodfellow GmbH, Bad Nauheim, Germany), fitting in a standard ESR quartz tube of 4 mm inner diameter. A step of 3 mm height was cut into the lower end of the rod so that there were two faces, one of half-circular shape perpendicular to the axis of the rod, the other of rectangular shape perpendicular to the first face. The crystal faces were aligned and glued to these two faces.

Axis Systems

Since the crystals were oriented with the aid of the $(40\bar{1})$ plane and the b-axis, the rotation patterns are described in a crystal coordinate system rsb in which r is perpendicular to the $(40\bar{1})$ plane, and s is normal to r and b. The axis system abc^* used in [1] derives from the monoclinic axis system abc with axis c replaced by the axis c^* perpendicular to the ab-plane. The components r and s of a vector in the rsb coordinate system transform to the abc^*-system by

$$\begin{pmatrix} a \\ c^* \end{pmatrix} = \begin{pmatrix} -\cos\alpha & \sin\alpha \\ \sin\alpha & \cos\alpha \end{pmatrix} \begin{pmatrix} r \\ s \end{pmatrix} \quad (1)$$

with $\alpha = 38.50°$. This transformation matrix is not identical with the standard matrix of rotation about the b-axis, since the order of the axes within the right-handed systems abc^* and rsb is interchanged.

Symmetry and Sites

There are four molecules per unit cell in KHCO$_3$, falling in two groups. The two members of each group are related by a center of inversion and thus are always magnetically equivalent. The two groups are transformed into each other by a twofold rotation parallel to the b-axis, and thus should split in the ESR spectra except when the field is in the rs-plane or along the b-axis. Since the rotation patterns show just this behaviour, the point group of pure KHCO$_3$ (2/m) is identical with that of the doped crystal which had to be expected because of the low copper content.

The rotation patterns were observed in the rs-, sb-, and br-planes by recording spectra in 5° increments. From these experiments the two minor principal axes of both the **g**- and **A**-tensor were found to lie in a plane perpendicular to the rs-plane and 65° off the s-axis. A fourth rotation pattern in that plane (henceforth called 65°-plane) was therefore recorded in order to obtain better estimates of the minor tensor components.

Since the spectra of the two sites split in the three planes perpendicular to the rs-plane, the problem of correct assignment of the hyperfine components to the two sites arises. This was solved by recording a rotation pattern with the rs-plane tilted by 45° relative to the rotation axis. The spectra of the two sites coalesced at 80° off the sb-plane, from which the corresponding hyperfine components in the spectra of the sb- and 65°-plane were assigned to the same site, with the assignment reversed in the br-plane. This assignment is based on the assumption that the patterns of the sites cross and not just touch at the point of coalescence, which appears justified from the symmetry by which the two sites are related.

In addition, the two outermost hyperfine lines of the spectra $(m_I = \pm 3/2)$ were assumed to belong to the same site. This must obviously be true for equal g-values but unequal hyperfine coupling of the sites. The rotation patterns in the br- and the 65°-plane practically fulfil this condition, from which the assignment is also clear in the sb-plane by way of the 45° pattern.

Fitting of Spectra

For improved spectral resolution, the individual positions of overlapping lines were calculated by simulation of the spectra with the third order expression which the detailed formulae of [7, 8] reduce to after introduction of the fitting parameters a_i

$$\begin{aligned} B_0 = B + a_1 m_I + (a_2/\mid a_2 \mid)(a_2 m_I)^2/B \\ + (a_3 m_I)^3/B^2 + (a_4/\mid a_4 \mid)a_4^2/B. \end{aligned} \quad (2)$$

In this expression for the magnetic field B of a hyperfine transition, m_I stands for the magnetic quantum number of the nucleus, and B_0 for the transition field of the pure Zeeman interaction. A further term $a_5 m_I/B^2$ was not found to be useful for fitting and was therefore neglected in the present case. The spectra were first order only in the vicinity of the largest hyperfine coupling in the rs-plane. Higher than second order terms were required in the plane of the two minor principal axes. The higher order was also obvious by weak forbidden lines appearing between the hyperfine transitions.

The Hamiltonian numerically fitted to the transition fields was the electron spin Zeeman plus the hyperfine interaction

$$\mathcal{H} = \beta B \cdot \mathbf{g} \cdot S + I \cdot \mathbf{A} \cdot S. \quad (3)$$

It was obviously not necessary to take further terms into account, like the nuclear Zeeman and quadrupole interaction.

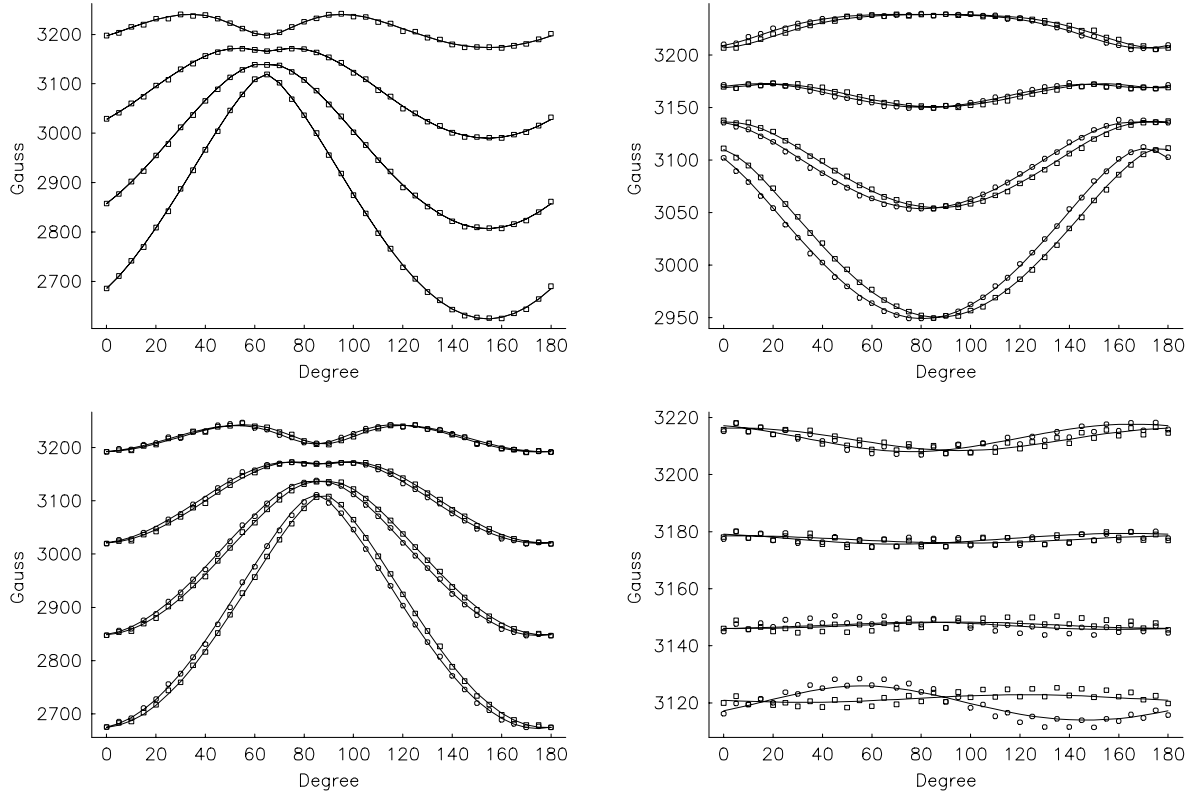Fig. 1. ESR rotation patterns for copper doped KHCO$_3$ single crystals. Top left: $rs = c^*a$-plane, $\nu = 9.0661$ GHz; top right: br-plane, $\nu = 9.0635$ GHz; bottom left: sb-plane, $\nu = 9.0648$ GHz; bottom right: $65°$-plane, $\nu = 9.0913$ GHz.

Table 1. Nominal (first line) and fitted (second line) initial direction of the magnetic field in the rotation patterns as given by the three angles θ_o, ϕ_o, and ω_o (see text). The numbers in parentheses are the standard deviations of the last digit(s) as obtained from the fitting procedure.

plane	θ_o	ϕ_o	ω_o	
rs	0	0	90	$B_0 \| s$
br	90	90	180	$B_0 \| b$
	88.4(6)	89.2(1)	183(1)	
sb	90	0	90	$B_0 \| s$
	96(2)	2.4(1)	91.2(8)	
$65°$	90	115	180	$B_0 \| b$
	88.8(1)	118.6(1)	181.6(14)	

The magnetic component of the rf field was always parallel to the rotation axis. Its direction in the crystal axis system rsb is given by the polar angle θ_o with respect to the b-axis, and the azimuthal angle ϕ_o in the rs-plane relative to the r-axis. The direction of the dc magnetic field, which was perpendicular to the rotation axis, must be specified by a third angle $\omega + \omega_o$ which measures the field's deviation from the plane formed by the rotation axis and the b-axis. The angle ω is the

abscissa in the rotation patterns and runs from $0°$ to $180°$. For each of the four patterns Table 1 lists the initial direction of the magnetic field in terms of the three angles θ_o, ϕ_o, and ω_o, and states which crystal axis it is parallel to.

From the definition of the initial angles θ_o, ϕ_o, and ω_o, the components of the dc magnetic field B_0 and of the rf field B_1 along the crystal axes are given by

$$B_r = B_0[\cos\theta_o \cos\phi_o \cos(\omega + \omega_o)$$
$$- \sin\phi_o \sin(\omega + \omega_o)] + B_1 \sin\theta_o \cos\phi_o,$$
$$B_s = B_0[\cos\theta_o \sin\phi_o \cos(\omega + \omega_o) \qquad (4)$$
$$+ \cos\phi_o \sin(\omega + \omega_o)] + B_1 \sin\theta_o \sin\phi_o,$$
$$B_b = -B_0 \sin\theta_o \cos(\omega + \omega_o) + B_1 \cos\theta_o.$$

Since small misalignments of the crystal are obvious from the spectra, the actual angles θ_o, ϕ_o, and ω_o for each rotation pattern except that in the rs-plane were treated as fitting parameters and proved to deviate only little from their nominal values (see Table 1).

Table 2. Principal values and principal axes of the **g**- and **A**(^{63}Cu)-tensor in copper doped KHCO$_3$.

g	a	b	c^*
2.0468(1)	−0.02(12)	1.00(1)	−0.02(1)
2.0474(1)	−0.437(8)	0.01(15)	0.899(8)
2.2347(1)	0.8993(3)	0.024(1)	0.4367(3)
A (mT)	a	b	c^*
2.63(2)	−0.433(2)	−0.096(22)	0.896(2)
3.22(1)	−0.065(17)	0.995(2)	0.075(15)
20.43(2)	0.8992(5)	0.026(1)	0.4367(4)

The tensors of both sites in the crystal axis system rsb are related by

$$\begin{pmatrix} t_{rr} & t_{rs} & t_{rb} \\ t_{rs} & t_{ss} & t_{sb} \\ t_{rb} & t_{sb} & t_{bb} \end{pmatrix} \xrightarrow{C_2(b)} \begin{pmatrix} t_{rr} & t_{rs} & -t_{rb} \\ t_{rs} & t_{ss} & -t_{sb} \\ -t_{rb} & -t_{sb} & t_{bb} \end{pmatrix}. \quad (5)$$

Thus the rotation patterns of both sites were fitted simultaneously with the same set of six parameters for the **g**- and **A**-tensors except for the necessary change of sign. The ^{65}Cu transitions were not included, since they had been found to fit to the third order expression (2) quite well. They thus do not contain additional information within experimental error. The FORTRAN computer program for the fitting was written by the author and makes use of standard mathematical subroutines from the NAG library (NAG Ltd, Oxford, UK). The good quality of the fit is shown in Figure 1.

The principal components and the principal axes of the tensors in the abc^*-axis system thus found are listed in Table 2. The axes with the largest principal value of both tensors are collinear and essentially lie in the c^*a-plane. While the principal axis of the **g**-tensor with the smallest principal value is parallel to the b-axis, the principal axis of the **A**-tensor with the second smallest principal value deviates somewhat from the direction of the b-axis. The higher order of the spectra obviously results from this deviation of the two minor principal axes of the **g**- and **A**-tensor from a common direction.

There is a principal ambiguity in the sign of one of the components of the principal axes [9] deriving from the unknown relative signs of the rotations. Since the point group of the crystals is 2/m, and the three rotation patterns in the planes perpendicular to the rs-plane can be mirrored at the twofold axis b, the sign ambiguity is irrelevant in the present case, since it just leads to an interchange in the labeling of the two sites.

Powder Pattern

The **g**- and **A**-tensors obtained from the single crystal experiments were used for the numerical simula-
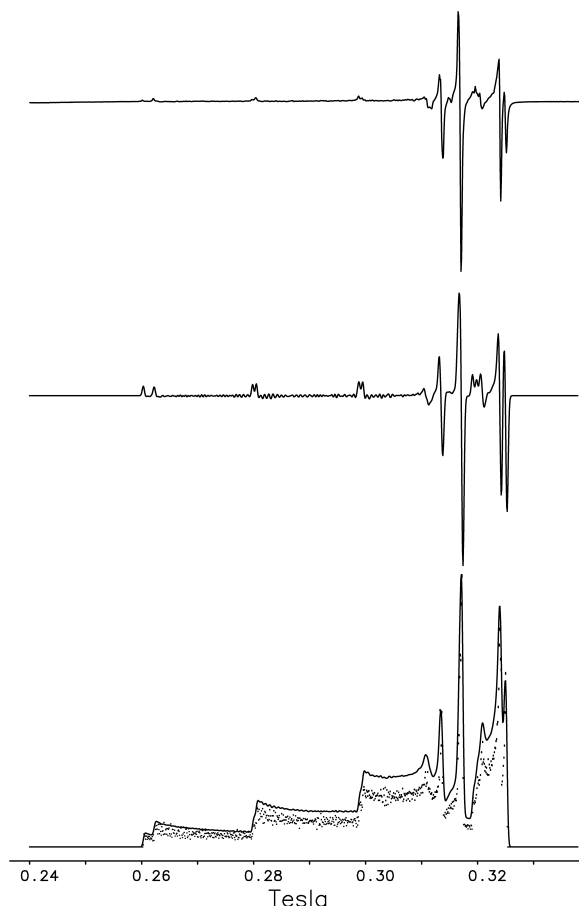

Fig. 2. Experimental (top) and simulated (center) powder pattern. Bottom: histogram of sampled points and convoluted absorption spectrum.

tion of the powder spectrum (program written by the author). 10,000 evenly spaced points on the hemisphere sampled the field directions and their associated transition fields. The absorption spectrum was obtained as a histogram with the intensities of the samples added up in sections of 1 Gauss width (Fig. 2, bottom, points). After convolution with a Gaussian function of 4 Gauss full width (Fig. 2, bottom, full line) the derivative spectrum was calculated (Fig. 2, center) which compares well with the experimental spectrum (Fig. 2, top), yet still contains some sampling noise.

From the simulation the right-most transition is identified as a ^{65}Cu hyperfine component, with all other major transitions in the $g_\perp$-range being ^{63}Cu signals. One of the $g_\perp$-transitions is of quite low intensity due to overlay with one $g_\parallel$-component.

Comparison of Results

There are obviously many similarities in the rotation patterns described here and in [1]. Differences can be seen in the behaviour of the two hyperfine components at higher field in the vicinity of the two splitting minima. A more important point is the assignment of the crystal faces. The patterns of [1] relate to the abc^*-axis system, which is transformed to the rsb-axis system of the present paper by rotation through $38.5°$ about the b-axis. Yet, the angles of the minimum in the rotation pattern in the $rs = c^*a$-plane differ by approximately $90°$ instead of $38.5°$, which led us to confirm our face assignment by X-ray diffraction (see above). It thus appears that the $(40\bar{1})$ face was misassigned in [1].

Furthermore, the smallest field for resonance and thus the largest g-value can be found in the c^*a-plane in both papers. Yet this is inconsistent with the g_{zz}-axis of [1] having its largest component along b. It is unclear whether there are only printing errors in the components of the principal axes of Table 1 in [1], since they do not form an orthogonal set.

The values 4.92 and 4.73 mT given for A_{xx} in [1] do not appear to conform with the spectra. The maximum and minimum principal values of a tensor correspond to the longest and the smallest diameter of the tensor ellipsoid. The ratio of the two values should therefore be larger than or equal to the ratio of the largest and the smallest interaction found in the spectra. The spectra of [1] show a largest splitting ratio of 5.2, whereas the A_{zz}/A_{xx}-ratios calculated from Table 1 of [1] are only 4.0 and 4.2 for the two sites. Since the present work additionally includes a rotation pattern in the plane of the two minor principal axes, it is expected to report more accurate values of the minor principal values and of the orientation of their axes.

Interpretation

The most natural assumption is that the Cu^{2+} ion replaces a potassium ion. These ions have eight oxygen atoms as their nearest neighbours [5]. Figure 3 shows this first coordination shell in two different perspectives. The c^*a-plane clearly is an approximate symmetry plane. If the two oxygen atoms with largest distance from this plane are neglected, there is approximate C_{2v}-symmetry. The unique principal axis of the g-tensor deviates by approximately $13°$ from the C_2-axis in the c^*a-plane due to the two oxygen atoms which disturb this symmetry. The deviation is just in the sense one would expect, since the two oxygen atoms and
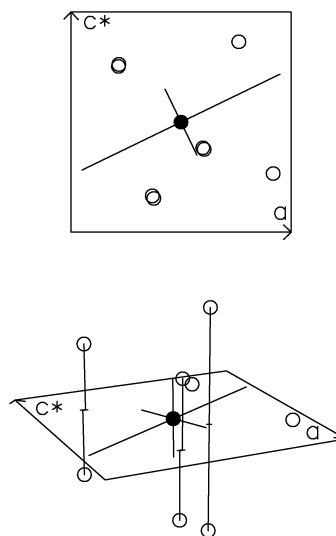

Fig. 3. Position of the K^+-ion (full circle), its first coordination shell of eight oxygens (open circles), and the experimental principal axes of the g-tensor in copper doped KHCO₃. Top: bird's eye view upon the ac^*-plane; bottom: perspective view.

the potassium atom form a triangle with likewise C_{2v}-symmetry, which forces a tensor axis perpendicular to the plane of the triangle. The resulting direction of the axes is a compromise between the requirements of the two partial structures of C_{2v}-symmetry.

The fact that the tensor principal axes fit the symmetry of the undisturbed potassium site is strong evidence for the substitution of potassium by Cu^{2+} ions without major disturbance of the first coordination shell.

Use as a Course Experiment

The interpretation by symmetry arguments in the preceding paragraph is also required from students in the course experiment which is performed in a considerably simplified manner. The **A**-tensor is not evaluated quantitatively, since this can not be done by elementary methods on account of the higher order of the spectra. The nondiagonal tensor elements g_{rb} and g_{sb} are smaller by more than a factor of 18 compared to g_{rs}, and smaller by more than a factor of 500 compared to the diagonal elements. They are therefore neglected, which means that a rotation pattern in the rs-plane only has to be measured. This also avoids the complication which the two sites give rise to, since they are magnetically equivalent in this plane. The spectra are simulated on a computer screen with a program which uses (2). The simulation renders B_0, from which g can be calculated. The **g**-tensor elements are obtained by fitting the data to

$$g^2 = g_{rr}\cos^2\theta + 2g_{rs}\cos\theta\sin\theta + g_{ss}\sin^2\theta, \quad (6)$$

see [10]. The direction of the unique principal axis of the **g**-tensor thus found usually deviates by just a few degrees from the value without that simplification.

Acknowledgements

[1] F. Köksal, I. Kartal, and B. Karabulut, Z. Naturforsch. **54a**, 177 (1999).

[2] M. Adams, M. S. Blois Jr, and R. H. Sands, J. Chem. Phys. **28**, 774 (1958).

[3] P. Groth, Chemische Krystallographie, Zweiter Teil, Die anorganischen Oxo- und Sulfosalze, Engelmann, Leipzig 1908.

[4] I. Nitta, Y. Tomiie, and C. H. Koo, Acta Cryst. **7**, 140 (1954).

[5] J. O. Thomas, R. Tellgren, and I. Olovsson, Acta Cryst. **B30**, 1155 (1974).

[6] J. O. Thomas, R. Tellgren, and I. Olovsson, Acta Cryst. **B30**, 2540 (1974).

[7] R. M. Golding and W. C. Tennant, Mol. Phys. **25**, 1163 (1973).

[8] R. M. Golding and W. C. Tennant, Mol. Phys. **28**, 167 (1974).

[9] D. S. Schonland, Proc. Phys. Soc. **73**, 788 (1959).

[10] J. A. Weil, J. R. Bolton, and J. E. Wertz, Electron Paramagnetic Resonance, Wiley, New York 1994, p. 89.